JSIAM Letters Vol.1 (2009) pp.68–71 ©2009 Japan Society for Industrial and Applied Mathematics JSIAM Letters

A hybrid of the optimal velocity and the slow-to-start models and its ultradiscretization

Kazuhito Oguma[1] and Hideaki Ujino[2]

Department of Mathematical Engineering and Information Physics, Faculty of Engineering, The University of Tokyo, 7-3-1 Hongo, Bunkyo-ku, Tokyo 113-8656, Japan[1]
Gunma National College of Technology, 580 Toriba, Maebashi, Gunma 371-8530, Japan[2]

E-mail *ujino@nat.gunma-ct.ac.jp*

Received August 24, 2009, Accepted October 6, 2009

Abstract

Through an extension of an ultradiscrete optimal velocity (OV) model, we introduce an ultradiscretizable traffic flow model, which is a hybrid of the OV and the slow-to-start (s2s) models. Its ultradiscrete limit gives a generalization of a special case of the ultradiscrete OV (uOV) model recently proposed by Takahashi and Matsukidaira. A phase transition from free to jam phases as well as the existence of multiple metastable states are observed in numerically obtained fundamental diagrams for cellular automata (CA), which are special cases of the ultradiscrete limit of the hybrid model.

Keywords optimal velocity (OV) model, slow-to-start (s2s) effect, ultradiscretization

Research Activity Group Applied Integrable Systems

1. Introduction

Studies on microscopic models for vehicle traffic provided a good point of view on the phase transition from free to congested traffic flow. Related self-driven many-particle systems have attracted considerable interests not only from engineers but also from physicists [1, 2]. Among such models, the optimal velocity model [3], which successfully shows a formation of "phantom traffic jams" in the high-density regime, is a car-following model describing an adaptation to the optimal velocity that depends on the distance from the vehicle ahead.

Whereas the OV model consists of ordinary differential equations (ODE), cellular automata (CA) such as the Nagel-Schreckenberg model [4], the elementary CA of Rule 184 (ECA184) [5], the Fukui-Ishibashi (FI) model [6] and the slow-to-start (s2s) model [7] are extensively used in analyses of traffic flow. Recently, Takahashi and Matsukidaira proposed a discrete OV (dOV) model, which enables an ultradiscretization of the OV model [8]. The resultant ultradiscrete OV (uOV) model includes both the ECA184 and the FI model as its special cases. However, the s2s effect remains to be included in their ultradiscretization. The aim of this letter is to present an ultradiscretizable hybrid of the OV and the s2s models.

2. The OV model and the s2s effect

Imagine many cars running in one direction on a single-lane highway. Let $x_k(t)$ denote the position of the k-th car at time t. No overtaking is assumed so that $x_k(t) \leq x_{k+1}(t)$ holds for arbitrary time t. The time-evolution of the OV model [3] is given by

$$\frac{dv_k(t)}{dt} = \frac{1}{t_0}\left[v_{\rm opt}\left(\Delta x_k(t)\right) - v_k(t)\right], \qquad (1)$$

where $v_k := dx_k/dt$ and $\Delta x_k := x_{k+1} - x_k$ are the velocity of the k-th car and the interval between the cars k and $k+1$, respectively. A function $v_{\rm opt}$ and a constant t_0 represent an optimal velocity and sensitivity of drivers, or the delay of drivers' response, in other words.

Since the current velocity and the current interval between the car ahead determine the acceleration through the time-evolution and the optimal velocity, we classify the OV model (1) as the acceleration-control type (aOV). On the other hand, the OV model of the velocity-control type (vOV) was proposed in earlier studies of the car-following models [9],

$$v_k(t) = v_{\rm opt}\left(\Delta x_k(t - t_0)\right). \qquad (2)$$

Replacement of t in the above equation (2) with $t + t_0$ and the Taylor expansion of $v_k(t + t_0)$ yield

$$\begin{aligned} v_{\rm opt}\left(\Delta x_k(t)\right) &= v_k(t + t_0) \\ &= v_k(t) + \frac{dv_k(t)}{dt}t_0 + \frac{1}{2}\frac{d^2v_k(t)}{dt^2}t_0^2 + \cdots, \end{aligned}$$

which is rewritten as

$$\frac{dv_k(t)}{dt} + \frac{1}{2}\frac{d^2v_k(t)}{dt^2}t_0 + \cdots = \frac{1}{t_0}\left[v_{\rm opt}\left(\Delta x_k(t)\right) - v_k(t)\right].$$

Thus the aOV model (1) is given by neglecting the higher order terms in the Taylor series (2). Though the aOV model is more common in the studies on vehicle traffic, we shall concentrate on an ultradiscretizable hybrid of the vOV and the s2s models. Thus we call the vOV model (2) simply as the OV model, hereafter.

Note that the input to the OV function $v_{\rm opt}(x)$ in the OV model (2) is the headway at a single point of time $t - t_0$ that is prior to the present time t. Thus we may say that the OV model describes, in a sense, "reckless"

drivers since the model pays no attention to the headway between the time $t-t_0$ and the present time t. On the other hand, "cautious" drivers governed by the s2s model [7] keep watching and require enough length of headway to go on for a certain period of time before they restart their cars. The contrast between the two models suggests the idea that the s2s effect and the OV model can be brought together by appropriately choosing an effective distance $\Delta_{\rm eff}x_k(t)$ containing information on the headway for a certain period of time going back from the present as an input to the OV function $v_{\rm opt}(x)$. We shall see this idea works in what follows.

What is crucial in the ultradiscretization of the aOV model [8] is the choice of the OV function,

$$v_{\rm opt}(x) := v_0\left(\frac{1}{1+{\rm e}^{-(x-x_0)/\delta x}} - \frac{1}{1+{\rm e}^{x_0/\delta x}}\right), \quad (3)$$

where v_0, x_0 and δx are positive constants. In terms of the auxiliary functions,

$$\widetilde{v}_{\rm opt}(x) := v_0\frac{d\tilde{x}_{\rm opt}(x)}{dx} \quad (4)$$

$$\widetilde{x}_{\rm opt}(x) := \delta x\log\left(1+{\rm e}^{(x-x_0)/\delta x}\right) \quad (5)$$

the OV function (3) is expressed as

$$v_{\rm opt}(x) = \widetilde{v}_{\rm opt}(x) - \widetilde{v}_{\rm opt}(x=0).$$

A naive discretization of the auxiliary function (4),

$$\widetilde{v}^{\rm d}_{\rm opt}(x) := \frac{\tilde{x}_{\rm opt}(x) - \tilde{x}_{\rm opt}(x-v_0\delta t)}{\delta t},$$

introduces the OV function for the discrete OV (dOV) model,

$$\begin{aligned} v^{\rm d}_{\rm opt}(x) &= \widetilde{v}^{\rm d}_{\rm opt}(x) - \widetilde{v}^{\rm d}_{\rm opt}(x=0) \\ &= \frac{\delta x}{\delta t}\log\left(\frac{1+{\rm e}^{(x-x_0)/\delta x}}{1+{\rm e}^{-x_0/\delta x}}\Big/\frac{1+{\rm e}^{(x-x_0-v_0\delta t)/\delta x}}{1+{\rm e}^{-(x_0+v_0\delta t)/\delta x}}\right), \end{aligned} \quad (6)$$

which is found to be ultradiscretizable [8].

Let $x^n_k := x_k(t=n\delta t)$ and $v^n_k := (x^{n+1}_k - x^n_k)/\delta t$ where $n(=0,1,2\cdots)$ and $\delta t(>0)$ are the integral time and the discrete time-step, respectively. Employing the effective distance as

$$\Delta^{\rm d}_{\rm eff}x^n_k := \delta x\log\left(\sum_{n'=0}^{n_0}\frac{{\rm e}^{-\Delta x^{n-n'}_k/\delta x}}{n_0+1}\right)^{-1}, \quad (7)$$

where $n_0 := t_0/\delta t$, we extend the OV model (2) in a time-discretized form as

$$v^n_k = v^{\rm d}_{\rm opt}\left(\Delta^{\rm d}_{\rm eff}x^n_k\right), \quad (8)$$

which is equivalent to

$$\begin{aligned} x^{n+1}_k &= x^n_k + \delta x\left\{\log\left[1+\left(\sum_{n'=0}^{n_0}\frac{{\rm e}^{-(\Delta x^{n-n'}_k - x_0)/\delta x}}{n_0+1}\right)^{-1}\right]\right. \\ &\quad \left. - \log\left[1+\left(\sum_{n'=0}^{n_0}\frac{{\rm e}^{-(\Delta x^{n-n'}_k - x_0 - v_0\delta t)/\delta x}}{n_0+1}\right)^{-1}\right]\right. \\ &\quad \left. - \log\left(1+{\rm e}^{-x_0/\delta x}\right) - \log\left(1+{\rm e}^{-(x_0+v_0\delta t)/\delta x}\right)\right\}. \end{aligned}$$

It is straightforward to confirm that the continuum limit $\delta t\to 0$ of the above discrete s2s–OV (ds2s–OV) model (8) reduces to the integral-differential equation which we call the s2s–OV model,

$$\begin{aligned} \frac{dx_k(t)}{dt} &= v_{\rm opt}\left(\Delta_{\rm eff}x_k(t)\right) \\ &= v_0\left(1+\frac{1}{t_0}\int_0^{t_0}{\rm e}^{-(\Delta x_k(t-t')-x_0)/\delta x}dt'\right)^{-1} \\ &\quad - v_0\left(1+{\rm e}^{x_0/\delta x}\right)^{-1}, \end{aligned} \quad (9)$$

where the corresponding effective distance is given by

$$\Delta_{\rm eff}x_k := \delta x\log\left(\frac{1}{t_0}\int_0^{t_0}{\rm e}^{-\Delta x_k(t-t')/\delta x}dt'\right)^{-1}.$$

We shall see that the s2s effect is indeed built into the OV model in the ultradiscrete limit of the ds2s–OV model.

3. Ultradiscretization

Ultradiscretization [10] is a scheme for getting a piecewise-linear equation from a difference equation via the limit formula

$$\lim_{\delta x\to+0}\delta x({\rm e}^{A/\delta x}+{\rm e}^{B/\delta x}+\cdots) = \max(A,B,\cdots).$$

In order to go forward to the ultradiscretization of the ds2s–OV model (8), it will be a good choice for us to begin with the ultradiscrete limit $\delta x\to+0$ of the auxiliary function (5):

$$\widetilde{x}^{\rm u}_{\rm opt}(x) := \lim_{\delta x\to+0}\widetilde{x}_{\rm opt}(x) = \max(0, x-x_0). \quad (10)$$

In the same way that the OV function for the dOV model (6) is obtained from the auxiliary function (5), we obtain the OV function for the uOV model [8] as

$$\begin{aligned} v^{\rm u}_{\rm opt}(x) &= \widetilde{v}^{\rm u}_{\rm opt}(x) - \widetilde{v}^{\rm u}_{\rm opt}(x=0) \\ &= \max\left(0, \frac{x-x_0}{\delta t}\right) - \max\left(0, \frac{x-x_0}{\delta t} - v_0\right), \end{aligned} \quad (11)$$

where $\widetilde{v}^{\rm u}_{\rm opt}(x) := (\widetilde{x}^{\rm u}_{\rm opt}(x) - \widetilde{x}^{\rm u}_{\rm opt}(x-v_0\delta t))/\delta t$. The effective distance (7), on the other hand, is ultradiscretized in the same manner:

$$\begin{aligned} \Delta^{\rm u}_{\rm eff}x^n_k &:= \lim_{\delta x\to+0}\Delta^{\rm d}_{\rm eff}x^n_k = -\max_{n'=0}^{n_0}\left(-\Delta x^{n-n'}_k\right) \\ &= \min_{n'=0}^{n_0}\left(\Delta x^{n-n'}_k\right). \end{aligned} \quad (12)$$

Thus we obtain an ultradiscrete equation

$$v^n_k = v^{\rm u}_{\rm opt}\left(\Delta^{\rm u}_{\rm eff}x^n_k\right), \quad (13)$$

which is equivalent to

$$\begin{aligned} x^{n+1}_k &= x^n_k + \max\left[0, \min_{n'=0}^{n_0}\left(\Delta x^{n-n'}_k\right) - x_0\right] \\ &\quad - \max\left[0, \min_{n'=0}^{n_0}\left(\Delta x^{n-n'}_k\right) - x_0 - v_0\delta t\right], \end{aligned}$$

as the ultradiscrete limit of the ds2s–OV model (8). We name it the ultradiscrete s2s–OV (us2s–OV) model. When the monitoring period n_0 is fixed at zero, the us2s–OV model reduces to a special case of the uOV model [8]. As we can see from (11), (12) and (13), the velocity v_k^n is determined by the optimal velocity for the minimum headway in the period between $n - n_0$ and n. Thus cars will not restart nor accelerate, unless enough clearance goes on for a certain period of time. On the other hand, cars immediately stop or slow down when their headways become too small to keep their velocities. The s2s effect and a "cautious" manner of driving are built into the uOV model in this way.

Now let us see how a CA comes out from the us2s–OV model. Let x_0 be the discretization step of the headway Δx_k^n, or equivalently, the size of the unit cell of the CA. Then with no loss of generality, we may set $x_0 = 1$. Assume that the number of vacant cells between the cars k and $k+1$, $\widetilde{\Delta} x_k^n := \Delta x_k^n - x_0$, must be non-negative, $\widetilde{\Delta} x_k^n \geq 0$, which prohibits car-crash. Then the us2s–OV model (13) reduces to

$$x_k^{n+1} = x_k^n + \min\left[\min_{n'=0}^{n_0}\left(\widetilde{\Delta} x_k^{n-n'}\right), v_0\delta t\right]. \qquad (14)$$

Fixing $v_0\delta t$ at an integer, we call this model the s2s–OV cellular automaton (CA). The s2s–OV CA reduces to the FI model [6] when $n_0 = 0$ and to the ECA184 [5] when $n_0 = 0$ and $v_0\delta t = 1 (= x_0)$. The s2s model [7] also comes out from the s2s–OV CA by choosing $n_0 = 1$ and $v_0\delta t = 1 (= x_0)$. Thus the s2s–OV CA is regarded as a hybrid of the FI model and an extended s2s model.

4. Numerical experiments

We shall numerically investigate the s2s–OV CA (14). Throughout this section, the length of the circuit L is fixed at $L = 100$ and the periodic boundary condition is assumed as well so that $x_k^n + L$ is identified with x_k^n.

Spatio-temporal patterns showing trajectories of each vehicle are given in Fig. 1. We choose the parameters and initial conditions so that jams appear in the trajectories. The two figures in the top share the same monitoring period $n_0 = 2$ but their maximum velocities are different. The top left trajectories show that the velocities of the vehicles are zero or one, which is less than or equal to its maximum velocity $v_0\delta t = 1$. In the top right trajectories whose maximum velocity $v_0\delta t = 3$, on the other hand, the velocities of the vehicles read zero, one, two and three. Thus we notice that the vehicles driven by the s2s–OV CA can run at any allowed integral velocity which is less than or equal to its maximum velocity $v_0\delta t$.

The other two figures in the bottom in Fig. 1 share the same maximum velocity $v_0\delta t = 2$, but their monitoring periods are different. As is observed in the bottom two figures, the longer the monitoring period is, the longer it takes for the cars to get out of the traffic jam. The jam front is observed to propagate against the stream of vehicles at constant velocity $x_0/\{(n_0+1)\delta t\}$, since cars have to wait $n_0 + 1$ time-steps to restart after their preceding cars restarted, as is depicted in Fig. 2.

Fig. 3 shows fundamental diagrams giving the relation

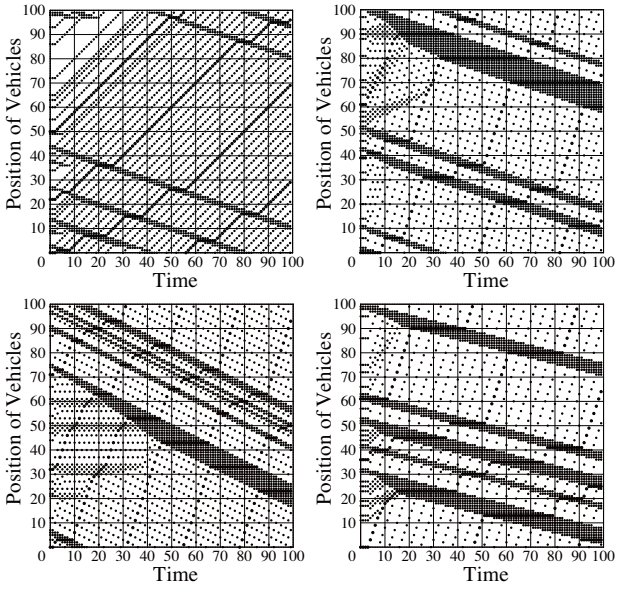

Fig. 1. The spatio-temporal patterns of the s2s–OV CA. For all four patterns, the number of cars K is fixed at $K = 30$. The maximum velocities $v_0\delta t$ and the monitoring periods n_0 for these patterns are (top left) $v_0\delta t = 1$, $n_0 = 2$, (top right) $v_0\delta t = 3$, $n_0 = 2$, (bottom left) $v_0\delta t = 2$, $n_0 = 1$ and (bottom right) $v_0\delta t = 2$, $n_0 = 3$, respectively.

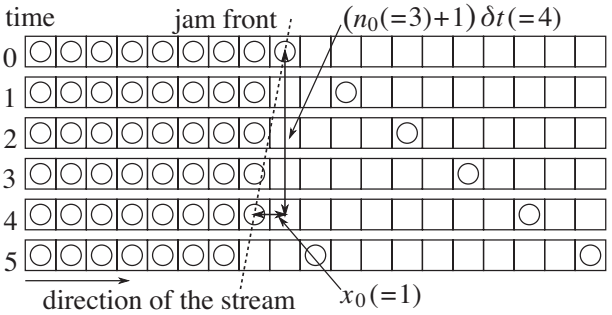

Fig. 2. Backward propagation of the jam front at constant velocity $x_0/\{(n_0+1)\delta t\} = 1/4$ for the case $v_0\delta t = 2$, $n_0 = 3$ and $x_0 = 1$.

between the vehicle flow

$$Q := \frac{1}{(n_1 - n_0 + 1)L}\sum_{k=1}^{K}\sum_{n=n_0}^{n_1}\frac{x_k^{n+1} - x_k^n}{\delta t},$$

which is equivalent to the total momentum of vehicles per unit length, and the vehicle density $\rho := K/L$, where K is the number of vehicles. The fundamental diagrams clearly show phase transitions from free to jam phases as well as metastable states, which are also observed in empirical flow-density relations [1,2]. It is remarkable that the fundamental diagrams have multiple metastable branches. This feature is similar to that reported by Nishinari *et al.* [11]. We observe that each fundamental diagram has $v_0\delta t$ metastable branches and a jamming line. The branches and the jamming line correspond to integral velocities that are less than or equal to the maximum velocity $v_0\delta t$. Let us confirm it with Fig. 3. The top two figures share the same monitoring period $n_0 = 3$, but their maximum velocities are different. The top left dia-

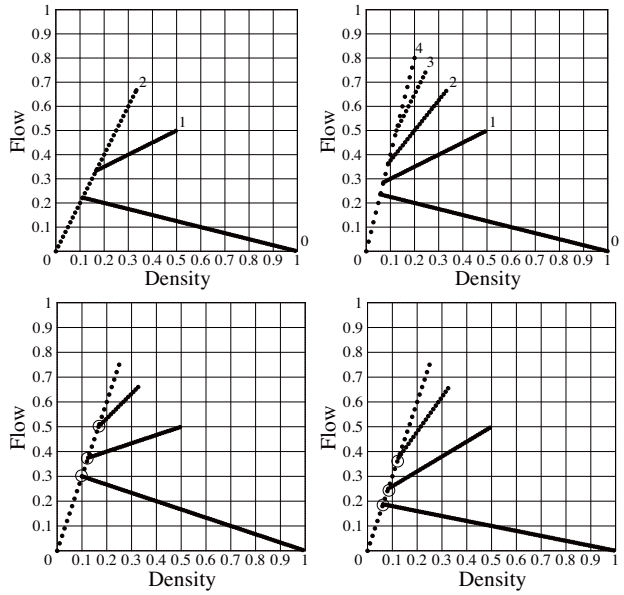

Fig. 3. The fundamental diagrams of the s2s–OV CA. The flows Q are computed by averaging over the time period $800 \leq n \leq 1000$. The maximum velocities $v_0\delta t$ and the monitoring periods n_0 for these patterns are (top left) $v_0\delta t = 2$, $n_0 = 3$, (top right) $v_0\delta t = 4$, $n_0 = 3$, (bottom left) $v_0\delta t = 3$, $n_0 = 2$ and (bottom right) $v_0\delta t = 3$, $n_0 = 4$, respectively. The inclination of the free line equals to the maximum velocity $v_0\delta t$. The jamming line has a negative inclination.

gram corresponding to $v_0\delta t = 2$ has three branches. This number equals to that of all the integral velocities, two, one and zero, as is depicted in the diagram. The number of the metastable branches in the top right diagram as well as those of the bottom two are explained in the same manner. This observation also suggests that the monitoring period is irrelevant to the number of metastable branches.

All the end points of the branches as well as the jamming line are on the line $\rho+Q(=\rho+Q(\delta t/x_0)) = 1$. This is because the density at the end point is the maximum density $\rho_{\max}(v)$ that allows the velocity of the slowest car to be $v\delta t$. The maximum density $\rho_{\max}(v)$ is determined by

$$\rho_{\max}(v) = \frac{x_0}{v\delta t + x_0}.$$

Since all the cars flow at the velocity $v\delta t$ when $\rho = \rho_{\max}(v)$, the corresponding flow is given by $Q(\rho_{\max}) = v\rho_{\max}$. Thus the relation $\rho_{\max} + Q(\rho_{\max})(\delta t/x_0) = 1$ holds.

The free line is a branch whose inclination equals to the maximal velocity $v_0\delta t$. Any other metastable branch and the jamming line branch out from the free line. We observe that the density at the branch point of the branch corresponding to the velocity $v\delta t$ reads

$$\rho_{\mathrm{b}} = \frac{x_0}{(v_0\delta t - v\delta t)n_0 + v_0\delta t + x_0}.$$

This observation is explained as follows. Suppose one car, say the car k, runs at the velocity v and the other $K-1$ cars run at the maximum velocity v_0. At the moment the k-th car slows down to v, the headway between the cars k and $k+1$ is $v\delta t + x_0$. Since it takes at least $n_0 + 1$ time-steps for the car k to speed up to v_0, the headway between the cars k and $k+1$ expands up to $H = (v_0\delta t - v\delta t)(n_0 + 1) + v\delta t + x_0 = x_0/\rho_{\mathrm{b}} \geq v_0\delta t$ by the time the k-th car speeds up to v_0. If all the cars can obtain the headway H, slow cars running at the velocity v disappear in the end. Thus the density at the branch point of the branch corresponding to the velocity $v\delta t$ is given by $\rho_{\mathrm{b}} = x_0/H$. Note that the density at the branch point becomes smaller as the monitoring period becomes larger.

5. Concluding remarks

Through an extension of the ultradiscrete OV model [8], we introduced the ds2s–OV (8) and s2s–OV (9) models as ultradiscretizable traffic flow models. The model is a hybrid of the OV [3] and the s2s [7] models whose ultradiscrete limit gives a generalization of a special case of the uOV model by Takahashi and Matsukidaira [8]. The phase transition from free to jam phases as well as the existence of multiple metastable states were observed in the numerically obtained fundamental diagrams for the s2s–OV CA (14), which are special cases of the us2s–OV model (13).

Detailed studies on the properties of the hybrid models (8), (9), (13) and (14) such as exact solutions, comparison with other traffic flow models as well as empirical data remain to be investigated.

Acknowledgments

The authors are grateful to D. Takahashi, J. Matsukidaira, A. Tomoeda, D. Yanagisawa and R. Nishi for their valuable comments at the spring meeting of JSIAM in March, 2009.

References

[1] D. Chowdhury, L. Santen and A. Schadschneider, Statistical physics of vehicular traffic and some related systems, Phys. Rep., **329** (2000), 199–329.
[2] D. Helbing, Traffic and related self-driven many-particle systems, Rev. Mod. Phys., **73** (2001), 1067–1141.
[3] M. Bando, K. Hasebe, A. Nakayama, A. Shibata and Y. Sugiyama, Dynamical model of traffic congestion and numerical simulation, Phys. Rev. E, **51** (1995), 1035–1042.
[4] K. Nagel and M. Schreckenberg, A cellular automaton model for freeway traffic, J. Physique I, **2** (1992), 2221–2229.
[5] S. Wolfram, Theory and applications of cellular automata, World Scientific, Singapore, 1986.
[6] M. Fukui and Y. Ishibashi, Traffic flow in 1D cellular automaton model including cars moving with high speed, J. Phys. Soc. Jpn., **65** (1996), 1868–1870.
[7] M. Takayasu and H. Takayasu, $1/f$ noise in a traffic model, Fractals, **1** (1993), 860–866.
[8] D. Takahashi and J. Matsukidaira, On a discrete optimal velocity model and its continuous and ultradiscrete relatives, JSIAM Letters, **1** (2009), 1–4.
[9] G. F. Newell, Nonlinear effects in the dynamics of car following, Oper. Res., **9** (1961), 209–229.
[10] T. Tokihiro, D. Takahashi, J. Matsukidaira and J. Satsuma, From soliton equations to integrable cellular automata through a limiting procedure, Phys. Rev. Lett., **76** (1996), 3247–3250.
[11] K. Nishinari, M. Fukui and A. Schadschneider, A stochastic cellular automaton model for traffic flow with multiple metastable states, J. Phys. A: Math. Gen., **37** (2004), 3101–3110.